

DYNAMICALLY DRIVEN EVOLUTION OF THE INTERSTELLAR MEDIUM IN M51

JIN KODA^{1,2}, NICK SCOVILLE¹, TSUYOSHI SAWADA³, MISTY A. LA VIGNE⁴, STUART N. VOGEL⁴, ASHLEY E. POTTS¹, JOHN M. CARPENTER¹, STUART A. CORDER¹, MELVYN C. H. WRIGHT⁵, STEPHEN M. WHITE⁴, B. ASHLEY ZAUDERER⁴, JENNY PATIENCE¹, ANNEILA I. SARGENT¹, DOUGLAS C. J. BOCK⁶, DAVID HAWKINS⁷, MARK HODGES⁷, ATHOL KEMBALL⁸, JAMES W. LAMB⁷, RICHARD L. PLAMBECK⁵, MARC W. POUND⁴, STEPHEN L. SCOTT⁷, PETER TEUBEN⁴, DAVID P. WOODY⁷

ABSTRACT

Massive star formation occurs in Giant Molecular Clouds (GMCs); an understanding of the evolution of GMCs is a prerequisite to develop theories of star formation and galaxy evolution. We report the highest-fidelity observations of the grand-design spiral galaxy M51 in carbon monoxide (CO) emission, revealing the evolution of GMCs vis-a-vis the large-scale galactic structure and dynamics. The most massive GMCs (Giant Molecular Associations - GMAs) are first assembled and then broken up as the gas flow through the spiral arms. The GMAs and their H₂ molecules are not fully dissociated into atomic gas as predicted in stellar feedback scenarios, but are fragmented into smaller GMCs upon leaving the spiral arms. The remnants of GMAs are detected as the chains of GMCs that emerge from the spiral arms into interarm regions. The kinematic shear within the spiral arms is sufficient to unbind the GMAs against self-gravity. We conclude that the evolution of GMCs is driven by large-scale galactic dynamics –their coagulation into GMAs is due to spiral arm streaming motions upon entering the arms, followed by fragmentation due to shear as they leave the arms on the downstream side. In M51, the majority of the gas remains molecular from arm entry through the inter-arm region and into the next spiral arm passage.

Subject headings: galaxies:individual (NGC5194, M51) — ISM: clouds — ISM: evolution

1. INTRODUCTION

Despite numerous studies of molecular gas in the Milky Way and galaxies (Scoville & Sanders 1987; Blitz et al. 2007), the processes affecting evolution of GMCs have remained poorly understood. In fact, uncertainty remains as to whether GMCs are stable structures that survive over a galactic rotation period ($> 10^8$ yrs; Scoville & Hersh 1979; Scoville & Wilson 2004) or are transient structures, destroyed immediately after formation by violent feedback from young stars [a few $\times 10^7$ yrs; Blitz & Shu 1980; Elmegreen 2007, or even shorter $\sim 10^6$ yrs; Elmegreen 2000; Hartmann, Ballesteros-Paredes & Bergin 2001].

The internal structure of GMCs is generally believed to be determined by an approximate balance of self-gravity and internal turbulent or magneto-turbulent pressures (exceeding the external ISM pressures by two orders of magnitude; Myers 1978). Therefore, GMCs are likely self-gravitationally bound, distinct, and long-lived objects (Scoville & Sanders 1987). A

difficulty, however, arises in maintaining the internal turbulence over the long lifetimes, since the turbulence should dissipate rapidly within a cloud crossing time (\sim a few $\times 10^6$ yrs). The energy must be continuously resupplied if their lifetimes are longer (e.g. Heitsch, Mac Low & Klessen 2001). The energy source is still unknown although supernovae and galactic rotation have been suggested (Mac Low & Klessen 2004; Wada, Meurer & Norman 2002; Koda et al. 2006). Models for rapid GMC formation and disruption have been proposed to avoid the need to re-energize the turbulence (Ballesteros-Paredes, Hartmann, Vazquez-Semadeni 1999). The absence of older > 5 Myr stellar populations within GMCs has been cited as evidence of short GMC lifetimes (Hartmann, Ballesteros-Paredes & Bergin 2001). However, more recent observations do find some older star populations (Jeffries 2007; Gandolfi et al. 2008; Oliveira et al. 2009), presumably indicating longer lifetimes. Moreover, at some point the older stars must drift free of the GMCs since they are no longer subject to the hydrodynamic forces of the ISM gas. The collapse timescale of star-forming cores via ambipolar diffusion is substantial, and may support the longevity (Tassis & Mouschovias 2004).

This controversy carries over when considering the galactic spatial distribution of GMCs, since early molecular line surveys of the Milky Way linked the GMC evolution to the Galactic disk dynamics. Cohen et al. (1980) argued that GMCs were confined largely to the spiral arms with very few seen in the inter-arm regions, implying that GMCs must be short-lived with a lifetime similar to the arm-crossing timescale (a few $\times 10^7$ yr; Dame, Hartmann & Thaddeus 2001). However, Sanders, Scoville & Solomon (1985) claimed to find many GMCs in the inter-arm regions, suggesting that the GMCs must be quasi-permanent structures, surviving

Electronic address: jin.koda@stonybrook.edu

¹ Department of Astronomy, California Institute of Technology, Pasadena, CA 91125

² Current address: Department of Physics and Astronomy, SUNY Stony Brook, Stony Brook, NY 11794-3800

³ Nobeyama Radio Observatory, National Astronomical Observatory, Nobeyama, Minamimaki, Minamisaku, Nagano, 384-1305, Japan

⁴ Department of Astronomy, University of Maryland, College Park, MD 20742

⁵ Department of Astronomy and Radio Astronomy Laboratory, University of California, Berkeley, CA 94720

⁶ Combined Array for Research in Millimeter-wave Astronomy, P. O. Box 968, Big Pine, CA 93513

⁷ Owens Valley Radio Observatory, California Institute of Technology, P. O. Box 968, Big Pine, CA 93513

⁸ National Center for Supercomputing Applications, University of Illinois at Urbana-Champaign, Champaign, IL 61820

$\gtrsim 10^8$ yrs, i.e. a substantial fraction of a galactic rotation period. A recent ^{13}CO survey suggests that GMCs in the inter-arm regions are less-massive (Koda et al. 2006; Jackson et al. 2006), accounting for the earlier discrepancies if the Cohen et al. survey missed the less-massive inter-arm GMCs. In any case, all Galactic surveys have the intrinsic limitation that the velocity dispersion and streaming motions of the clouds can blur out the spiral arm/inter-arm definition when the disk is viewed edge-on.

High-resolution molecular gas observations of external face-on spiral galaxies are therefore essential for the full census of GMC population over galactic disks. However, prior interferometers, which are required for such high-resolution imaging, had only a small number of telescopes, and thus were severely limited by low image-fidelity. Indeed, the high side-lobes of bright spiral arms due to poor uv -coverage have often led to false structures in the inter-arm regions (Rand & Kulkarni 1990; Aalto et al. 1999; Helfer et al. 2003).

2. OBSERVATIONS AND DATA REDUCTION

High-fidelity imaging of nearby galaxies at millimetre-wavelengths has now become feasible with the Combined Array for Research in Millimeter Astronomy (CARMA). CARMA is a new interferometer, combining the six 10-meter antennas of the Owens Valley Radio Observatory (OVRO) millimeter interferometer and the nine 6-meter antennas of the Berkeley-Illinois-Maryland Association (BIMA) interferometer. The increase to 105 baselines (from 15 and 45 respectively) enables the highest fidelity imaging ever achieved at millimeter wavelengths. The entire optical disk of the Whirlpool galaxy M51 ($6.0' \times 8.4'$) was mosaiced in 151 pointings with Nyquist sampling of the 10m antenna beam (FWHM of 1 arcmin for the 115GHz CO J=1-0 line). The data were reduced and calibrated using the Multichannel Image Reconstruction, Image Analysis, and Display (MIRIAD) software package (Sault, Teuben & Wright 1995).

We also obtained total power and short spacing data with the 25-Beam Array Receiver System (BEARS) on the Nobeyama Radio Observatory 45m telescope (NRO45, FWHM = $15''$). Using the On-The-Fly observing mode (Sawada et al. 2008), the data were oversampled on a $5''$ lattice and then re-gridded with a spheroidal smoothing function, resulting in a final resolution of $22''$. We used the NOSTAR data reduction package developed at the Nobeyama observatory. We constructed visibilities by de-convolving the NRO45 maps with the beam function (i.e. a convolution of the $15''$ Gaussian and spheroidal function), and Fourier-transforming them to the uv -space. We combined the CARMA and NRO45 data in Fourier space, inverted the uv data using theoretical noise and uniform weighting, and CLEANed the maps to yield a three-dimensional image cube (Right Ascension, Declination, and LSR Doppler velocity).

The combined data have an RMS sensitivity of 40 mJy/beam in 5.1 km s^{-1} wide channels, corresponding to $1 \times 10^5 M_\odot$ at the distance of 8.2 Mpc (adopting a CO-to- H_2 conversion factor of $X_{\text{CO}} = 2 \times 10^{20} \text{ cm}^{-2} [\text{K km s}^{-1}]^{-1}$). Typical GMCs in the Milky Way (i.e. $4 \times 10^5 M_\odot$ in mass and 40 pc in diameter, Scoville & Sanders 1987) are therefore detected at 4σ significance. Our angular resolution of $4''$ corresponds to

160 pc, which is high enough to isolate (but not resolve) the GMCs, given that the typical separation of Galactic GMCs is a few 100 pc to kpc (Scoville & Sanders 1987; Koda et al. 2006). The combination of spatial resolution, sensitivity, and image-fidelity differentiates our study from previous work (Vogel, Kulkarni & Scoville 1988; Garcia-Burillo, Guerin & Cernicharo 1993; Nakai, Kuno & Sofue 1994; Aalto et al. 1999; Helfer et al. 2003), and enables a reliable census of GMCs in M51.

Figure 1a shows the CO map integrated over all velocities. The new image shows the full distribution of molecular gas over the entire optical disk of M51 ($14.3 \times 20.0 \text{ kpc}^2$), including both the prominent spiral arms and inter-arm regions. The bright inner arms have been previously imaged (Vogel, Kulkarni & Scoville 1988; Aalto et al. 1999), but the new data extend these arms over the full disk and most importantly, yield significant detection of inter-arm GMCs for the first time. Figure 2a shows the distribution of discrete GMCs measured using CLUMPFIND (Williams, de Geus & Blitz 1994), clearly indicating many GMCs with mass exceeding $4 \times 10^5 M_\odot$ in the inter-arm regions. Lower mass GMCs would not be detected by the cloud finding algorithm and only 36% of the inter-arm CO emission is seen in the detected discrete clouds shown in Figure 2.

3. DISCUSSION

Two possibilities for GMC formation and lifetime can clearly be distinguished from the observed GMC distribution relative to the spiral arms. One possibility is that they are transient, short-lived structures – formed locally at convergence locations of the galactic hydrodynamic flows and destroyed quickly by disruptive feedback from star formation within the GMCs. Alternatively, if the GMCs are long-lived, lasting through the inter-arm crossing period, their presence in the inter-arm regions is naturally explained. A simple calculation can be done to rule out the formation of abundant GMCs from the ambient gas with a low average-density in the inter-arm regions. Assuming a very ideal spherical gas accretion of the converging velocity v into the volume with the radius r , the mass accumulates within the time t is $M = 4\pi r^2 v m_{\text{H}} n t$, where n is the number density of ambient gas and m_{H} is the mass of hydrogen atom. Using a GMC radius $r \sim 20 \text{ pc}$, typical velocity dispersion in galactic disk $v \sim 10 \text{ km s}^{-1}$, and average gas density $n \sim 1 - 5 \text{ cm}^{-3}$ (inferred for M51 in the areas without GMCs), it takes $\sim 10^8$ yrs to accumulate $4 \times 10^5 M_\odot$. This mass-flow argument is valid even when the ambient gas is not exactly diffuse but consists of smaller clouds if their distribution is roughly uniform. Therefore, the majority of the GMCs in the inter-arm regions cannot have formed there locally on the required short timescales (i.e. inter-arm crossing timescale $\sim 10^8$ yrs).

Figure 2a also reveals that the molecular gas properties, specifically their masses, are significantly dependent on galactic environment. The most massive structures with $10^7 - 8 M_\odot$, referred to as GMAs, are found only in spiral arms, not in inter-arm regions. The improved image fidelity was necessary to avoid misidentification of even such massive GMAs, especially in the inter-arm regions. GMAs must therefore form and disrupt while crossing the spiral arms (with a timescale

typically $\sim 2\text{-}5 \times 10^7$ yrs). Their formation within the arms is aided by the spiral streaming which causes deflection and convergence of the galactic flow streamlines in the arms. Although stellar feedback (e.g. photo-dissociation by OB star ultraviolet radiation and supernova explosions) is often invoked for GMC destruction (Larson 1987; Williams & McKee 1997), these mechanisms are not a likely cause of significant GMA dissipation given their masses ($10^7\text{-}8M_\odot$, see Figure 2a; Williams & McKee 1997). More telling is the high mass fraction of H_2 in the inter-arm regions (Figure 2b,c). Comparing the mean molecular gas surface density with that of the HI (Braun et al. 2007), we estimate that 70-80% of the gas remains H_2 within the major part of the disk (~ 12 kpc; Figure 2c). Thus, GMAs are not significantly dissociated into atomic or ionized gas. We conclude that the GMAs must be fragmented into the less-massive GMCs and the most massive of these are seen as discrete clouds in the inter-arm regions in Figure 2a. Figure 2a includes only the GMCs down to the 4σ level; the sum of their emission is 36% of the total emission of the entire disk. The remainder of molecular emission is presumably in less-massive GMCs, not identified as discrete clouds at the current resolution and sensitivity. Their distribution must be roughly uniform in the inter-arm regions since they are resolved out at $4''$ resolution.

It is unlikely that a significant portion of the remaining emission arises in diffuse molecular gas at low densities. First, the critical density for collisional-excitation of CO(J=1-0) transition is a few $\times 100\text{cm}^{-3}$ in optically thick clouds, similar to the average density within GMCs in the Milky Way (Scoville & Sanders 1987). The critical density is even higher, $\sim 3000\text{cm}^{-3}$, in optically thin regions. Thus, CO emission should not be detected if the density is lower than the densities of GMCs. Secondly, CO molecules rapidly dissociate in the diffuse interstellar radiation field if they are unshielded by a sufficient column of dust. It is often discussed that a visual extinction of only $A_V \sim 1$ mag is sufficient for shielding (Pringle, Allen & Lubow 2001); however, this is true only at high densities (10^3cm^{-3} ; van Dishoeck & Black 1988). A higher A_V is necessary at lower densities, since the rate of molecular formation must be rapid to counterbalance the rapid dissociation. At the typically densities of a few 10^2cm^{-3} expected for molecular gas based on Galactic studies, several mag of visual extinction are required and the CO emitting gas must reside in GMC-like structures during passage through the inter-arm areas.

Lastly, we address the nature of the GMAs: are they distinct clouds, and simply an extension of GMC mass spectrum, or the confusion of many GMCs concentrated by orbit crowding in the spiral potential but unresolved due to the limited spatial resolution. The gas surface densities within the GMAs is $200\text{-}1000M_\odot\text{pc}^{-2}$, generally higher than that in Galactic GMCs ($\sim 170M_\odot\text{pc}^{-2}$; Solomon et al. 1987). The FWHM thickness of the molecular gas disk in M51 is unknown but in the Galaxy it is ~ 120 pc (Scoville & Sanders 1987), so the average gas densities within the GMAs ($40\text{-}200\text{cm}^{-3}$) are similar to typical GMC densities (Solomon et al. 1987). Thus, the molecular gas would continuously fill the entire volume within GMAs. We conclude that the GMAs are most likely not just confusion of multiple GMCs, but instead must be discrete structures. The GMCs coag-

ulate and form GMAs in spiral arms. Such mass concentrations would be susceptible to kinematic fragmentation in high shear gradients across the spiral arms. In fact, the shear gradients are $200\text{-}600\text{km s}^{-1}\text{kpc}^{-1}$ (Figure 1b), large enough to pull apart the GMAs against their self-gravity; the shear timescale, defined as the inverse of Oorts A-constant, is comparable to the free-fall timescale ($\sim 5\text{-}10$ Myr). In addition the GMAs in our images are in virtually all instances elongated along the spiral arms, instead of the round shapes expected if they are strongly self-gravitating. Formation of massive GMAs without an aid of gravity is seen in theoretical models due to GMC agglomeration in the spiral density wave (Dobbs & Bonnell 2006), and due to hydrodynamic instabilities triggered by strong shear upon entering the spiral arms (Wada & Koda 2004; Wada 2008).

The remnants of fragmented GMAs are seen in the inter-arm regions. Optical and infrared images show spur structures emerging from the spiral arms into the inter-arm regions (La Vigne, Vogel & Ostriker 2006) as dark filamentary lanes originating on the outside (downstream) of spiral arms (Figure 3). A few spurs have also been detected in CO line (Corder et al. 2008) and in Figure 3 here. They are formed by fragmentation of GMAs leaving the arms into the inter-arm regions. With the observed shear motions, GMAs would naturally shear into such filamentary spur structures. The total masses of spurs are a few $\times 10^6\text{-}7M_\odot$, approaching the masses of typical GMAs ($\sim 10^7M_\odot$).

These new observations suggest that the evolution of the dense ISM in M51 is dynamically driven. The GMCs coalesce into GMAs as they flow into the spiral arms and the cloud orbits converge in the spiral arm. The very massive GMA seen in the spiral arms must have lifetimes comparable to the time needed to cross the arms ($\sim 2 - 5 \times 10^7$ yrs). On leaving the spiral arms, these GMAs are fragmented by the strong shear motions and then ejected into the downstream inter-arm regions as lower mass GMCs. Our new observations reveal over a hundred of the most massive GMCs ($> 4 \times 10^5M_\odot$) in the interarm regions. These GMCs are detected throughout the interarm areas and therefore must have lifetimes comparable with the interarm crossing time of 10^8 yrs. The majority of the interarm molecular gas is not resolved at our current detection limit $\sim 4 \times 10^5M_\odot$ – thus the fragmentation of GMAs must proceed to even lower mass GMCs. It is clear that most of the molecular gas is converted not simply to HI but to GMCs, since the molecules dominate the overall gas abundance in the major part of the disk (central ~ 12 kpc). The lifetimes of the lower mass GMCs require more sensitive observations.

We thank an anonymous referee for thoughtful comments. Support for CARMA construction was derived from the Gordon and Betty Moore Foundation, the Eileen and Kenneth Norris Foundation, the Caltech Associates, the states of California, Illinois, and Maryland, and the National Science Foundation. Ongoing CARMA development and operations are supported by the National Science Foundation under a cooperative agreement, and by the CARMA partner universities. This research is partially supported by HST-AR-11261.01.

REFERENCES

- Aalto, S., Huttemeister, S., Scoville, N. Z., Thaddeus, P. A. 1999, *ApJ*, 522, 165
- Ballesteros-Paredes, J., Hartmann, L. & Vazquez-Semadeni, E. 1999, *ApJ*, 527, 285
- Blitz, L. & Shu, F. H. 1980, *ApJ*, 238, 148
- Blitz, L., Fukui, Y., Kawamura, A., Leroy, A., Mizuno, N., Rosolowsky, E. 2007, *Protostars and Planets V.*, p. 81
- Braun, R., Oosterloo, T. A., Morganti, R., Klein, U. & Beck, R. 2007, *A&A*461, 455
- Corder, S., Sheth, K., Scoville, N. Z., Koda, J., Vogel, S. N. & Ostriker, E. 2008, *ApJ*, 689, 148
- Cohen, R. S., Cong, H., Dame, T. M. & Thaddeus, P. 1980, *ApJ*, 239, 53
- Dame, T. M., Hartmann, D. & Thaddeus, P. 2001, *ApJ*547, 792
- Dobbs, C. L. & Bonnell, I. A. 2006, *MNRAS*, 367, 873
- Elmegreen, B. G. 2000, *ApJ*, 530, 277
- Elmegreen, B. G. 2007, *ApJ*, 668, 1064
- Gandolfi, D., Alcalá, J. M., Leccia, S. et al. 2008, *ApJ*, 687, 1303
- García-Burillo, S., Guerin, M., Cernicharo, J. 1993, *A&A*, 274, 123
- Hartmann, L., Ballesteros-Paredes, J. & Bergin, E. A. 2001, *ApJ*, 562, 852
- Heitsch, F., Mac Low, M. -M., & Klessen, R. S. 2001, *ApJ*, 547, 280
- Helfer, T. T., Thornley, M. D., Regan, M. W., Wong, T., Sheth, K., Vogel, S. N., Blitz, L. Bock, D. C. J. 2003, *ApJS*, 145, 249
- Jackson, J. M. Rathborne, J. M., Shah, R. Y. et al. 2006, *ApJS*, 163, 145
- Jeffries, R. D. 2007, *MNRAS*, 381, 1169
- Koda, J., Sawada, T., Hasegawa, T. & Scoville, N. Z. 2006, *ApJ*, 638, 191
- Larson, R. B. 1987, *NATO ASI Series* 232, 459
- La Vigne, M. A., Vogel, S. N. & Ostriker, E. C. 2006, *ApJ*, 650, 818
- Mac Low, M. -M. & Klessen, R. S. 2004, *Reviews of Modern Physics*, 76, 125
- Myers, P. C. 1978, *ApJ*, 225, 380
- Nakai, N., Kuno, N., Handa, T. Sofue, Y. 1994, *PASJ*46, 527
- Oliveira, I., Merin, B., Pontoppidan, K. M., et al. 2009, *ApJ*, 691, 672
- Pringle, J. E., Allen, R. J. & Lubow, S. H. 2001, *MNRAS*, 327, 663
- Rand, R. J. & Kulkarni, S. R. 1990, *ApJ*, 349, 43
- Sanders, D. B., Scoville, N. Z. & Solomon, P. M. 1985, *ApJ*, 289, 373
- Sault, R. J., Teuben, P. J., Wright, M. C. H. 1995, *ASP Conference Series* 77, 433
- Sawada, T., Ikeda, N., Sunada, K. et al. 2008, *PASJ*, 60, 445
- Scoville, Z. & Hersh, K. 1979, *ApJ*, 229, 578
- Scoville, N. Z. & Sanders, D. B. 1987, *Astrophysics and space science library* 134, 21
- Scoville, N. Z. & Wilson, C. D. 2004, *ASP Conference series*, 322, 245
- Solomon, P. M., Ravilo, A. R., Barrett, J. & Yahil, A. 1987, *ApJ*, 319, 730
- Tassis, K. & Mouschovias, T. C. 2004, *ApJ*, 616, 283
- van Dishoeck, E. F. & Black, J. H. 1988, *ApJ*, 334, 771
- Vogel, S. N., Kulkarni, S. R. & Scoville, N. Z. 1988, *Nature*334, 402
- Wada, K., Meurer, G. & Norman, C. 2002, *ApJ*, 577, 197
- Wada, K. & Koda, J. 2004, *MNRAS*, 349, 270
- Wada, K. 2008, *ApJ*, 675, 188
- Williams, J. P., de Geus, E. J. & Blitz, L. 1994, *ApJ*, 428, 693
- Williams, J. P. & McKee, C. F. 1997, *ApJ*, 476, 166

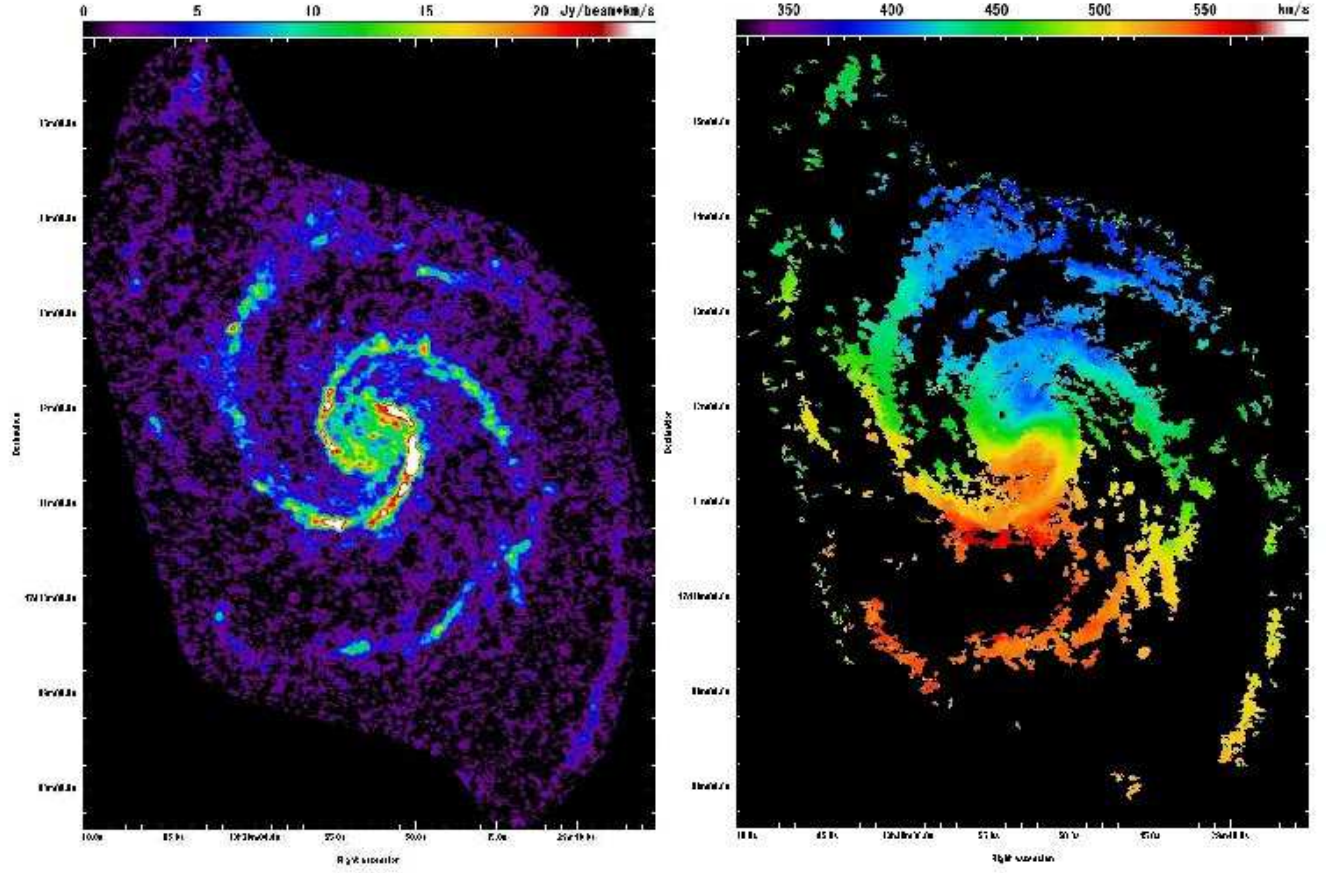


FIG. 1.— (a) Integrated intensity map of CO(J=1-0) emission of the entire disk of M51. The $6.0' \times 8.4'$ region was mosaiced in 151 pointings at $4''$ resolution with the CARMA interferometer. The total power and short-spacing data are obtained with the On-The-Fly mapping mode of the BEARS multi-beam receiver on the Nobeyama Radio Observatory 45m telescope (NRO45). The CARMA and NRO45 data are combined in the Fourier space. The map clearly detect GMCs over the entire disk for the first time, including both the prominent spiral arms and inter-arm regions. (b) Velocity field. Significant shear motions are seen at tangential positions (PA of the disk kinematic major axis is -11deg)

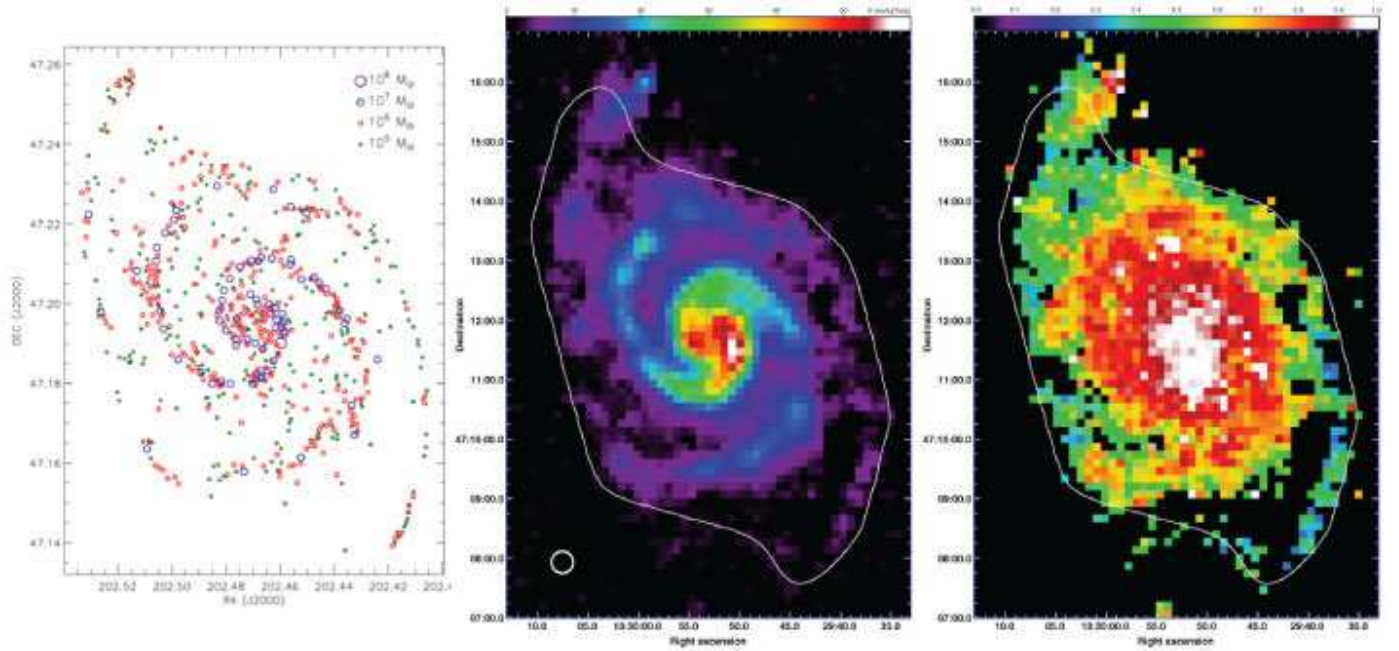


FIG. 2.— (a) Distribution of GMCs ($10^5 - 10^6 M_\odot$) and giant molecular associations (GMAs; $> 10^7 M_\odot$) in M51. The GMCs/GMAs are identified with the CLUMPFIND algorithm (Williams, de Geus & Blitz 1994), down to 4σ significance, corresponding to the typical GMC mass in the Milky Way ($4 \times 10^5 M_\odot$; Scoville & Sanders 1987). The small green circles includes only the GMCs with mass above $4 \times 10^5 M_\odot$. The GMAs are seen only in the spiral arms, suggesting that they are assembled and broken up as the gas flows through the spiral arms. Numerous GMCs are still seen in the inter-arm regions, indicating that they survive while crossing the inter-arm regions. (b) Nobeyama 45 m telescope CO($J=1-0$) map. The circle at the lower-left corner is the $22''$ beam. The white contour around the emission indicates roughly the coverage of CARMA observations. (c) Molecular gas fraction defined as $2n_{H_2}/(n_H + 2n_{H_2})$, calculated with H_I data from Braun et al. (2007). The fraction is high within the major part of the disk and does not change azimuthally, indicating that the gas stays molecular over a revolution.

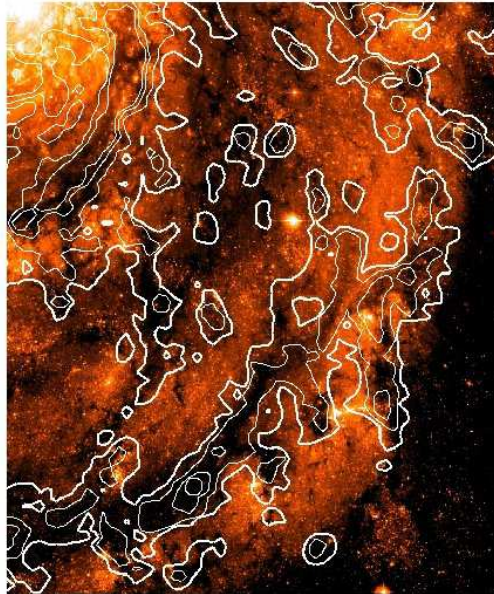


FIG. 3.— Spurs in inter-arm regions. Spurs that originate from the spiral arms and extend into the inter-arm regions are seen as optical extinction in the B -band image from the *Hubble Space Telescope* (*HST*) archive (color). Molecular gas (contours) traces the spurs, possibly the fragmented remnants of GMAs. Contours are at 3, 5, 9, 13 σ in each velocity channel, and the lowest contour is presented with a thick line. The spurs have very narrow line widths and are seen clearly in channel maps, but not as much in an integrated intensity map. We therefore overlaid the contours of all channels with emission exceeding 3σ .